

Analysis of Overload Shedding (OLS) - Adaptive Defense Scheme (ADS) on the 150 KV Priok Subsystem to Enhance The Reliability of Jakarta's Electricity Supply In N-1/N-2 Contingency Scenarios

¹Mochammad Ali Randy, ²Rinaldy Dalimi

^{1,2}Departement of Electrical Engineering, Faculty of Engineering

^{1,2}University of Indonesia

Depok, Indonesia

E-mail: ¹mochammad.ali31@ui.ac.id, ²rinaldy@eng.ui.ac.id

Abstract—This study analyses the implementation of Overload Shedding (OLS) and Adaptive Defense Scheme (ADS) in the 150 kV Priok subsystem to enhance Jakarta's electricity supply reliability under N-1/N-2 contingency scenarios. Using DigSILENT PowerFactory, the research evaluates system stability by modelling dynamic load responses, power flows, and contingency simulations. The objective is to optimize OLS-ADS parameters to mitigate cascading failures and ensure equipment safety during critical faults. The methodology involves detailed modelling of the Priok subsystem, including generators, transformers, and protective relays, validated via power flow analysis using the Newton-Raphson method. N-1/N-2 contingencies—such as tripping of IBT2/Bekasi, IBT1/Cawang, and dual IBT failures—are simulated to assess OLS-ADS performance. Dynamic load shedding logic adapts to real-time system conditions, prioritizing critical loads and generators. Results show that OLS-ADS successfully prevents equipment overloading in N-1 scenarios (e.g., IBT2/Bekasi tripping) by shedding 6–20% of the load, maintaining voltages (0.9–1.0 pu) and frequencies (49.9–50 Hz) within safe limits. Rotor angles in Priok's PLTGU units remain below IEEE's $\pm 90^\circ$ threshold. However, N-2 contingencies (e.g., simultaneous loss of IBT2/4/Bekasi) require shedding 50% of the load to avert cascading failures, highlighting systemic vulnerabilities. The study concludes that OLS-ADS significantly improves N-1 resilience but underscores the need for enhanced redundancy (e.g., integrating Muara Tawar's 500/150 kV IBTs) to mitigate N-2 risks. Findings provide actionable guidelines for optimizing ADS logic and expanding grid infrastructure to ensure reliable power supply in DKI Jakarta.

Keywords: Overload Shedding, Adaptive Defence Scheme, Power System Reliability, N-1/N-2 Contingency, DigSilent.

I. INTRODUCTION

The reliability and security of 500 kV and 150 kV system operations in Java-Bali are crucial because they directly impact the stability and economic value of the power system. Major disturbances that cause widespread blackouts can result in significant financial losses due to lost revenue from electricity sales. Therefore, a reliable and secure operating system is a top priority, even if it requires higher costs to meet operational constraints, such as operating less economic power plants.

To achieve a secure operating system, PLN UIP2B identifies the types and locations of disturbances that could potentially cause widespread blackouts. This identification involves in-depth system studies, including analysis of oscillation phenomena and dynamic simulations. One effort to improve system reliability is the implementation of an Adaptive Defense Scheme (ADS), which is more flexible than conventional schemes because it can dynamically adjust protection settings [4].

However, to ensure the effectiveness of ADS, accurate and comprehensive testing is required. DigSILENT, as a dynamic power system simulation tool, provides an effective solution for analyzing the

ADS response under various operational scenarios, including N-1/N-2 contingencies [5]. This tool enables in-depth evaluation of ADS performance, including the system's ability to perform Overload Shedding (OLS) to prevent cascading failures.

This research focuses on analyzing the OLS-ADS scheme in the Priok 150 kV subsystem to improve power transfer reliability in DKI Jakarta. Using DigSILENT, dynamic simulations will be conducted to evaluate the system's response to various disturbances and to optimize the OLS and ADS parameters. The results of this research are expected to provide accurate and effective implementation recommendations, which can serve as a reference for improving the reliability of the Java-Bali power system. Based on the description of the problem above, the author is interested in developing this research more deeply, in accordance with the research objectives that have been set.

II. RESEARCH METHODS

The research process consists of five distinct stages: 150 kV Priok Subsystem Topology, Data Preparation, Experimentation, Modeling, and Model Evaluation.

$$Q_{act} = Q_0 * \left[a_Q * \left(\frac{V_{act}}{V_{nom}} \right)^2 + b_Q * \left(\frac{V_{act}}{V_{nom}} \right)^1 + c_Q * \left(\frac{V_{act}}{V_{nom}} \right)^0 \right] * (1 + K_{qf} * \Delta f) \dots (2)$$

The parameter values a, b, d, and K were calculated using the percentage data of load types per substation, as presented in Table 3. Each percentage of these load types was multiplied by the load model parameters obtained from reference papers [7], as shown in Table 4.

Tabel 4. Dynamic Parameters of Load Type Models

	P(v)			Q(v)			Kpf	Kqf
	P	I	Z	P	I	Z		
Residensial	0	0.8	0.2	-0.6	0.4	1.2	0.8	-2.2
Publik/Komersial	0.4	0.2	0.4	-1	0.6	1.4	1.2	-1.6
Industri	0.8	0.2	0	-3.7	2	2.7	2.6	1.6

The calculated load parameter values for each substation are presented in Table 5.

Tabel 5. Calculated Load Parameters

No	Load Transformer	P(v)			Q(v)			Kpf	Kqf
		aP(P)	bP(I)	cP(Z)	aQ(P)	bQ(I)	cQ(Z)		
1	ANCOL TRAF0 #1	0.32	0.20	0.48	1.65	0.87	-1.51	1.47	-0.99
2	ANCOL TRAF0 #2	0.15	0.20	0.65	2.22	1.49	-2.71	2.09	0.43
3	ANCOL TRAF0 #3	0.12	0.20	0.68	2.30	1.57	-2.88	2.17	0.62
4	CEMPAKA PUTIH TRAF0 #1	0.29	0.26	0.45	1.68	0.90	-1.58	1.48	-0.92
5	CEMPAKA PUTIH TRAF0 #2	0.35	0.29	0.36	1.45	0.65	-1.10	1.22	-1.50
6	BEKASI TRAF0 #1	0.21	0.73	0.05	1.25	0.45	-0.70	0.87	-2.07
7	BEKASI TRAF0 #2	0.26	0.55	0.19	1.35	0.56	-0.91	1.04	-1.78
8	BEKASI TRAF0 #3	0.28	0.50	0.21	1.35	0.55	-0.90	1.05	-1.79
9	BEKASI TRAF0 #4	0.30	0.41	0.29	1.42	0.63	-1.04	1.15	-1.59
10	BEKASI TRAF0 #5	0.29	0.48	0.23	1.36	0.57	-0.93	1.07	-1.75

90	SETIA BUDI TRAF0 #2	0.22	0.20	0.58	1.98	1.22	-2.20	1.82	-0.18
91	SETIA BUDI TRAF0 #3	0.24	0.20	0.56	1.93	1.17	-2.10	1.77	-0.30
92	RAWA KUNING TRAF0 #1	0.38	0.22	0.40	1.43	0.64	-1.07	1.23	-1.52
93	RAWA KUNING TRAF0 #2	0.36	0.25	0.40	1.47	0.68	-1.15	1.26	-1.44
94	RAWA TERATE TRAF0 #1	0.32	0.20	0.48	1.65	0.87	-1.51	1.47	-0.99
95	RAWA TERATE TRAF0 #2	0.15	0.20	0.65	2.22	1.49	-2.71	2.09	0.43
96	RAWAMANGUN TRAF0 #1	0.35	0.32	0.33	1.39	0.59	-0.97	1.15	-1.66
97	RAWAMANGUN TRAF0 #2	0.28	0.23	0.49	1.73	0.96	-1.69	1.55	-0.78
98	IG TSBV SUNBARSEON, LINE KOC TRANSI HALIM	0.15	0.20	0.65	2.22	1.49	-2.71	2.09	0.43
99	PADEMANGAN TRAF0 #1	0.30	0.41	0.28	1.41	0.61	-1.02	1.14	-1.62
100	PADEMANGAN TRAF0 #2	0.24	0.66	0.10	1.26	0.46	-0.72	0.91	-2.03

2.2 Experiment

The objective of this research is to identify credible N-1/N-2 contingencies and vulnerabilities within Bekasi 24, Cawang 1, and Priok Subsystems, which serve as the primary electricity supply, impacting system and subsystem security in the DKI Jakarta capital region. In these experiments, contingency simulations will be performed using Power Factory DigSILENT software [8]. Ultimately, this research aims to recommend Adaptive Defense Scheme protection designs capable of mitigating widespread disturbances in the Java-Bali system with layered security measures.

2.3 Modelling

To analyze the implementation of the adaptive defense scheme and its impact on operational reliability, the 150 kV Priok Subsystem was modeled in

detail using DigSILENT PowerFactory software. DigSILENT PowerFactory was chosen for its comprehensive capabilities in modeling power systems, including power flow analysis, fault studies, transient stability analysis, and real-time simulation [9]. Furthermore, DigSILENT PowerFactory is widely used in the power industry and academia, ensuring high validity and credibility of the simulation results obtained [10].

The modeling of the 150 kV Priok Subsystem in DigSILENT PowerFactory includes an accurate representation of the system's main components, including [5][11]:

- **Generators:** Generator units connected to the 150 kV Priok Subsystem were modeled with appropriate parameters, including generation capacity, capability curves, governor parameters, and exciters.
- **Transformers:** 150/20 kV power transformers and interbus transformers were modeled with impedance data, tap ratios, and saturation characteristics.
- **Transmission Lines:** 150 kV transmission lines were modeled with line parameters such as series impedance, shunt admittance, and line length.
- **Loads:** Loads in the 150 kV Priok Subsystem were modeled as static or dynamic loads, depending on data availability. Historical load data was used to represent realistic load profiles.
- **Protection Equipment:** Protection relays, including distance relays, overcurrent relays, and frequency relays, were modelled to facilitate the analysis of existing protection schemes and the implementation of the adaptive defense scheme.
- **Control Systems:** The model also includes Automatic Voltage Regulators (AVR) and Power System Stabilizers (PSS).

Data for the modeling was obtained from various sources, including 150 kV Priok Subsystem single line diagrams (SLD), equipment technical data from manufacturers, protection relay settings, and historical operational data from PLN. These data were input into DigSILENT PowerFactory to create an accurate and representative model of the actual system conditions [12].

The developed model was then validated by comparing power flow and fault simulation results with measurement data or historical data from the real system. This validation is crucial to ensure that the model accurately represents the system and can be used for further analysis. Figure 2. shows the single line diagram of the 150kV Priok subsystem modeled in DigSILENT

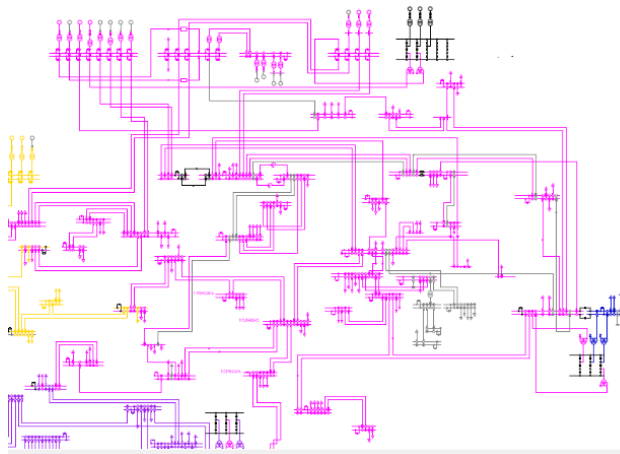


Figure 2. 150 kV Priok Subsystem Modeled in DigSILENT

With the accurate 150 kV Priok Subsystem model in DigSILENT PowerFactory, in-depth analysis of N-1/N-2 contingency scenarios, adaptive defense scheme implementation, and protection parameter optimization can be effectively performed. Simulation results from DigSILENT PowerFactory will serve as the primary basis for evaluating system performance and formulating recommendations for enhancing operational reliability.

2.4.1 Power Flow Simulation of the 150 kV Priok Subsystem Using DigSILENT Software.

To evaluate performance and identify potential vulnerabilities within the 150 kV Priok Subsystem, a power flow simulation was conducted using DigSILENT PowerFactory software [5][13], as illustrated in Figure 3. This simulation aimed to determine voltage conditions at each bus, active and reactive power flow in each line and transformer, and to validate the developed system model.

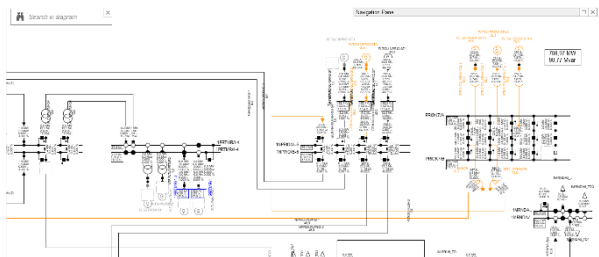


Figure 3. 150 kV Priok Subsystem Power Flow

The power flow simulation was performed using the Newton-Raphson method [12][14], a widely used iterative technique for solving nonlinear power flow equations. This method was chosen due to its rapid convergence and ability to handle complex systems. The convergence tolerance employed was 0.0001 per unit (pu) for both active and reactive power.

2.4.2 Initial Value

After all load data, generation data, and transmission line data were input into DigSILENT, and following the successful execution of the power flow without errors and achieving converged data, the RMS values for the total load at each Interbus Transformer (IBT) were obtained, as presented in Table 6.

Tabel 6. Initial Value

List of IBTs	Digsilent Calculated Value			In (A)	Equivalent In to MW	OLS Settings		OCR Settings	
	Peak (MW)	Average (MW)	Low Load (MW)			I set = 1.1 * In (A)	Equivalent Iset to MW	I set = 1.2 * In (A)	Equivalent Iset to MW
IBT Bekasi#2	255,7352	234,1257	146,1736	1718	350	1889,8	390	2300	470
IBT Bekasi#4	247,3065	226,5634	131,1159	1718	350	1889,8	390	2300	470
IBT Cawang#1	258,3111	238,3543	144,1532	1718	350	1889,8	390	2300	470
IBT Priok#1	347,9573	364,1554	280,5889	1718	350	1889,8	390	2300	470
Total	1109,31	1063,199	702,0316	1718	350	1889,8	390	2300	470

As shown in Table 6, the peak load value is 1109.31 MW; the average load value is 1063.199 MW, and the low load value is 702 MW. The maximum OLS IBT value is 110%*In for each IBT, equivalent to ±390 MW.

2.4 Model Evaluation

2.4.1 Power Flow Analysis

Power flow analysis is a fundamental aspect of power system planning and operation, aimed at determining the distribution of active and reactive power, voltages, and phase angles at each bus within the network, as defined by equations (3) and (4) [15]. The basic power flow equations, involving nonlinear relationships between line admittances, voltage magnitudes, and phase angles, form the core of this analysis. In practice, the use of software such as DigSILENT PowerFactory enables accurate and efficient modeling to solve these equations, both in normal operating conditions and under disturbance scenarios such as N-1 or N-2 contingencies. With the ability to integrate advanced numerical methods like Newton-Raphson, this software not only simplifies the calculation process but also provides deep insights into the behavior of power systems under various operational conditions

$$P_i = \sum_{j=1}^N V_i V_j Y_{ij} \cos(\theta_{ij} - \delta_i + \delta_j) \dots (3)$$

$$Q_i = \sum_{j=1}^N V_i V_j Y_{ij} \sin(\theta_{ij} - \delta_i + \delta_j) \dots (4)$$

with

- P_i, Q_i : Active and reactive power at the bus i
- V_i, V_j : Voltage magnitudes at buses i and j
- Y_{ij} : Line admittance between buses i and j
- θ_{ij} : Transmission line impedance angle
- δ_i, δ_j : Voltage phase angles at buses i and j
- N : Total number of buses in the system

2.4.2 Non-Linear Power Flow Formulation

The power flow equations are nonlinear due to the product of variables V_i , V_j , and trigonometric functions (cos and sin). To solve these equations, it is necessary to segregate known and unknown variables based on bus type [16]:

1. Bus Slack (Reference Bus):

- Voltage (V) and phase angle (δ) are known.
- Used as a calculation reference.

2. Bus PV (Generator Bus):

- Active power (P_i) and voltage magnitude (V_i) are known.
- Phase angles (δ_i) and reactive power (Q_i) are calculated.

3. Bus PQ (Load Bus):

- Active power (P_i) and reactive power (Q_i) are known.
- Voltage magnitudes (V_i) and phase angles (δ_i) are calculated.

2.4.3 Newton-Raphson Method

The Newton-Raphson method is employed to solve nonlinear power flow equations by iteratively approximating the solution [17]. The mathematical formulation steps are as follows:

a. Mismatch Equations

In equation (5) and (6), define the error (ΔP_i and ΔQ_i) between the calculated power and the known power [2]:

$$\Delta P_i = P_i^{spec} - P_i^{calc} \dots (5)$$

$$\Delta Q_i = Q_i^{spec} - Q_i^{calc} \dots (6)$$

with

P_i^{spec}, Q_i^{spec} : Known (specified) active and reactive power.

P_i^{calc}, Q_i^{calc} : Active and reactive power calculated based on current estimates.

b. Jacobian Matrix

The Jacobian matrix (J), as shown in equation (7), is used to relate changes in errors (ΔP_i , ΔQ_i) to changes in variables ($\Delta \delta_i$, ΔV_i) [18]:

$$\begin{bmatrix} \Delta P \\ \Delta Q \end{bmatrix} = \begin{bmatrix} \frac{\partial P}{\partial \delta} & \frac{\partial P}{\partial V} \\ \frac{\partial Q}{\partial \delta} & \frac{\partial Q}{\partial V} \end{bmatrix} \cdot \begin{bmatrix} \Delta \delta \\ \Delta V \end{bmatrix} \dots (7)$$

with

$\frac{\partial P}{\partial \delta}$: Partial derivative of active power with respect to phase angle.

$\frac{\partial P}{\partial V}$: Partial derivative of active power with respect to voltage magnitude.

$\frac{\partial Q}{\partial \delta}$: Partial derivative of reactive power with respect to phase angle.

$\frac{\partial Q}{\partial V}$: Partial derivative of reactive power with respect to phase angle.

Following the definition of the mathematical equations (3), (4), (5), (6), and (7), the next step is to perform the Newton-Raphson iterations.

c. Newton-Raphson Iteration

The iteration process is performed until the error (ΔP_i , ΔQ_i) approaches zero. The steps are as follows:

1. Variable Initialization

- Initial phase angle estimation (δ_i) dan Voltage magnitude (V_i).

2. Calculating Actual Power:

- Calculate P_i^{calc} and Q_i^{calc} based on the current estimate.

3. Calculating Errors:

- Calculate ΔP_i and ΔQ_i based on the current estimate.

4. Update Variables:

- Employ the Jacobian matrix for updating estimations:

$$\begin{bmatrix} \Delta \delta \\ \Delta V \end{bmatrix} = J^{-1} \cdot \begin{bmatrix} \Delta P \\ \Delta Q \end{bmatrix} \dots (8)$$

5. Repeat Iteration:

- Repeat steps 2-4 until the error reaches the specified tolerance (ϵ).

2.4.4 Over Load Shedding (OLS) Static and Dynamic (ADS)

Overload Shedding (OLS) is understood as the excessive loading of conductors or transformers. This occurs due to excessive consumer load demand being handled by the equipment, necessitating load shedding to reduce the loading within permissible limits. OLS does not address dynamic stability issues within the system. The defense scheme for OLS can be designed to be either static or dynamic in relation to its target [19].

a. Determining OLS Current Settings

OLS settings consist of current and time parameters. Current settings must consider the capacity and lifespan of transformers/conductors, average loading, ambient temperature, and safety margins. Therefore, OLS settings for transformers or conductors are set at 110% of the nominal current, with a reset current of 85% or

adjusted according to other protection performance or agreements between asset owners.

- The nominal current refers to the minimum current capacity of transformers/conductors operating in series within the equipment, as declared by the asset owner.
- Time settings can be definite. Definite time settings for OLS are adjusted to a time range that can be derived from coordination with other protection. The first stage delay time starts from 2-3 seconds or shorter, depending on coordination with other protection.
- Inverse time settings for OLS can be used under certain conditions that do not allow for the use of definite time settings alone, such as overload conditions with high current during N-2 or higher contingency scenarios as shown in Figure 4 [20].

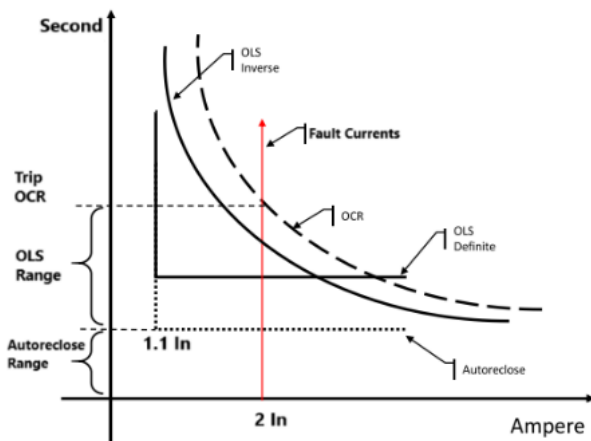


Figure 4. Static OLS Operating Time Range

b. Determining ADS Current Settings

The dynamic OLS planning stages are similar to static OLS planning, with the key difference being the determination of OLS logic. In static OLS, the load quota and target defense scheme are fixed, whereas in dynamic OLS, the load quota and targets can adapt to system conditions according to the established OLS logic. OLS logic is used for processing measurement/status data as OLS operation inputs and for determining the selection and amount of load to be shed.

In Dynamic OLS (Adaptive Defense Scheme), which utilizes contingency/event-based analysis within this power flow simulation study, all contingencies to be accommodated are defined, along with the mitigation measures to be implemented based on equipment responses observed during the power flow study.

In the dynamic OLS setting, using a base contingency defined by circuit breaker statuses, the base parameters are permitted to operate without a time delay/instantaneously, as illustrated in Figure 5 [20].

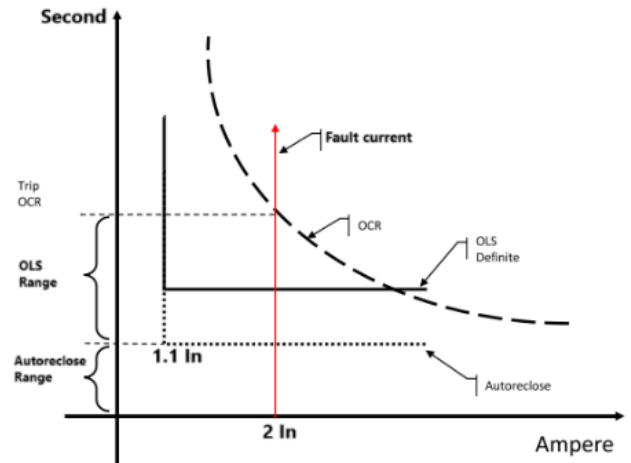


Figure 5. ADS Operating Time Range

2.4.5 Defence Scheme Design

There are two types of adaptive defense schemes: event-based and parameter-based. Assuming a subsystem is supplied by M generators and N Interbus Transformers (IBTs), as shown in Figure 6, and considering the system's topology (T), where T is 1 if included in the system and 0 if not, and the Circuit Breaker (CB) status (C), where C is 1 if closed and 0 if open, the need for load shedding/generation shedding can be calculated based on equation (8).

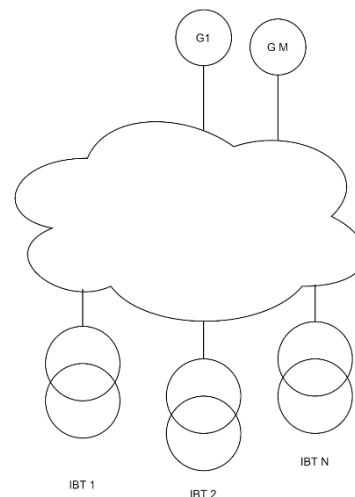


Figure 6. ADS Subsystem Modeling

$$\begin{aligned}
 P_{cut} &= \left\{ \sum cap \right. \\
 &- \sum P_{no-trip} \\
 &- \sum trip, \text{ if the value is negative ... (9)}
 \end{aligned}$$

with

- P_{cut} : Load/Generation Shedding to be Performed
- Cap : Remaining line or IBT capacity
- P_{trip} : Active power from the disrupted line or IBT
- $P_{no-trip}$: Active power of undisturbed lines or IBTs

III. RESULT AND ANALYSIS

3.1 N-1 Contingency Simulation

The following analysis examines the outcomes of N-1 contingency tests conducted with two separate schemes. This examination seeks to assess the system's capacity to uphold stability and power supply quality when a key component, specifically an IBT (Inter Bus Transformer), is lost.

3.1.1 Tripping of IBT 2 Bekasi with Parallel Operation of IBT 4 Bekasi

This test was conducted during peak load on October 30, 2024, when the total substation (SS) load was 1109.3101 MW, and the SS Priok generation load was 1358.4848 MW. In this simulation, IBT#2 Bekasi was tripped at time $t_1 = 1.06$ s with a load of 255.7352 MW. Consequently, the load on IBT#4 Bekasi, which is parallel to IBT#2, increased to 390.428 MW at $t_2 = 1.3$ s, as illustrated in Figure 7. This triggered the OLS relay to send an arming signal to the ADS controller. At time $t_3 = 1.5$ s, the load on IBT#4 exceeded its maximum limit of $1.1 \times I_n$, which is 419.0238 MW, as illustrated in Figure 8, prompting the controller to immediately execute OLS on the Bekasi IBT load by shedding 60.6899 MW. This resulted in a load of 362.4744 MW on IBT#4 Bekasi, equivalent to a loading of 0.9 per unit (pu)

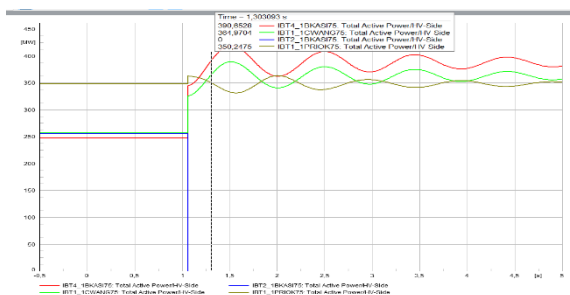


Figure 7. OLS Relay IBT#2 Bekasi Start to Send

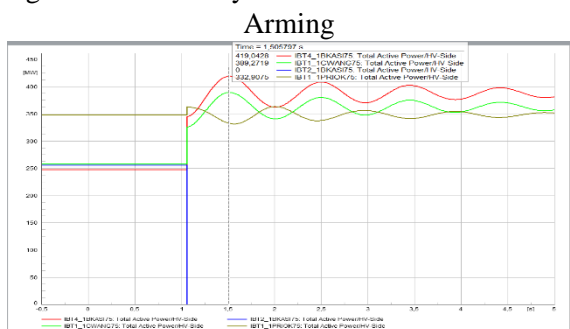


Figure 8. IBT#2 Reaches Maximum Loading

The voltage and frequency values occurring at each substation with a vulnerability index within the 150 kV Priok Subsystem, both pre- and post-fault, remained within the safe range: 0.9 pu to 1 pu for voltage, and 49.9 Hz during the fault, returning to 50 Hz upon system recovery, as illustrated in Figures 9 and 10.

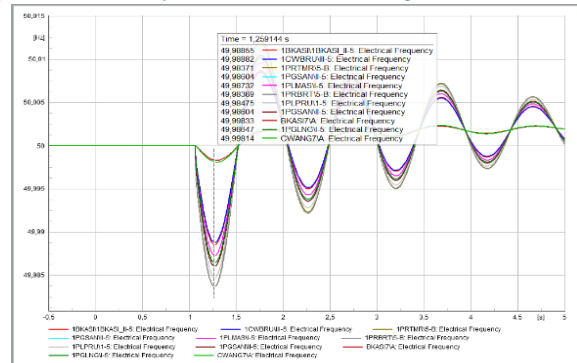


Figure 9. Voltage Values at Substations with a Vulnerability Index > 0.5

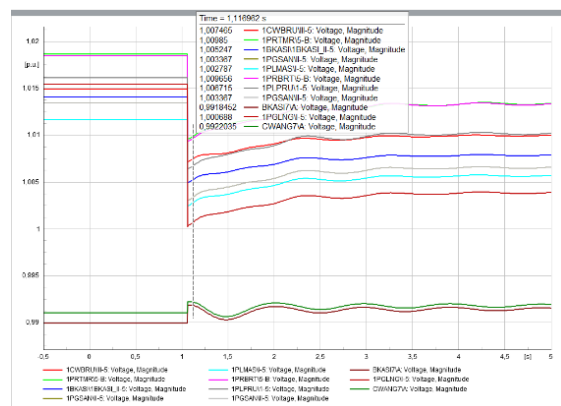


Figure 10. Frequency Values at Substations with a Vulnerability Index > 0.5

This simulation also considers the rotor angle for all Priok generators at 14:00 on October 30, 2024, specifically Combine Cycle Block 1 at 1.30 degrees, Combine Cycle Block 3 at 2.0 degrees, and Full Combine Cycle Block 4 at 1.20 degrees. According to IEEE C37.118.1 standards, the rotor angle variations observed in all these combined cycle power plants can be deemed safe for operation, as the variation range is at most 3 degrees. This is illustrated in Figure 11.

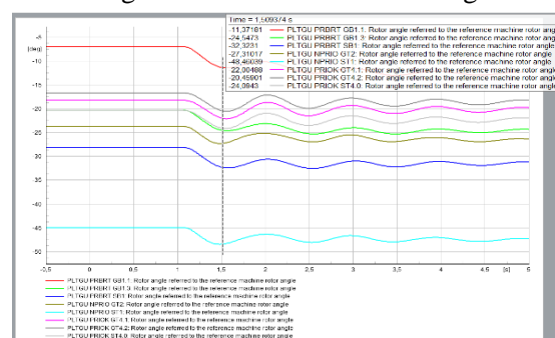


Figure 11. Rotor Angles at Priok Generation

Simulations were also conducted under peak load, average load, and low load conditions. Under average and low load conditions, no Load Shedding was activated, as the load remained adequately distributed among the Bekasi IBT, Cawang IBT, and Priok IBT, as demonstrated in Table 7.

Tabel 7. Load Condition Contingency N-1 Simulation

Load Condition	Total Load SS Priok (MW)	Total Priok SS Generation (MW)	Power Loss (N-1 IBT Bekasi) (MW)	OLS (MW)	Final Beban SS (MW)
Peak Load	1109,3101	1358,4848	255,7352	60,6899	1048,6202
Average Load	1063,1988	1169,83872	234,1257	0	1063,1988
Low Load	702,0316	884,14685	146,1736	0	702,0316

3.1.2 Tripping of IBT 1 Cawang

The N-1 contingency simulation testing of IBT 1 Cawang is a unique test, as IBT 1 Cawang in the 150 kV Priok Subsystem is not configured in parallel like IBT 2 and 4 Bekasi. Consequently, the effect of IBT 1 Cawang tripping resulted in a 258.311 MW load transfer at $t_1 = 1.06$ s. This load distribution shifted to IBT 2 and 4 Bekasi, which before the IBT 1 Cawang disturbance had loads of 255.7352 MW and 247.3065 MW, respectively. At $t_2 = 1.339$ s, the OLS relay of IBT 4 Bekasi first sent an arming signal to the ADS controller, due to the IBT 4 Bekasi loading reaching 398.6694 MW. Subsequently, at $t_3 = 1.374$ s, IBT 2 Bekasi loading also sent an arming signal to the ADS controller, as shown in Figure 12. However, at $t_4 = 1.5$ s, both Bekasi IBTs experienced a load surge, exceeding the tolerance threshold of $1.1 \cdot I_n$, or above 400 MW, as depicted in Figure 13. Consequently, the ADS relay immediately commanded load shedding of loads on IBT 2 and 4 Bekasi, totaling 205.9939 MW. Following the load shedding, at $t_5 = 2.963$ s, the load returned to 358.4118 MW, equivalent to 0.919 pu for IBT 4, and 358.1037 MW, equivalent to 0.918 pu for IBT 2 Bekasi.

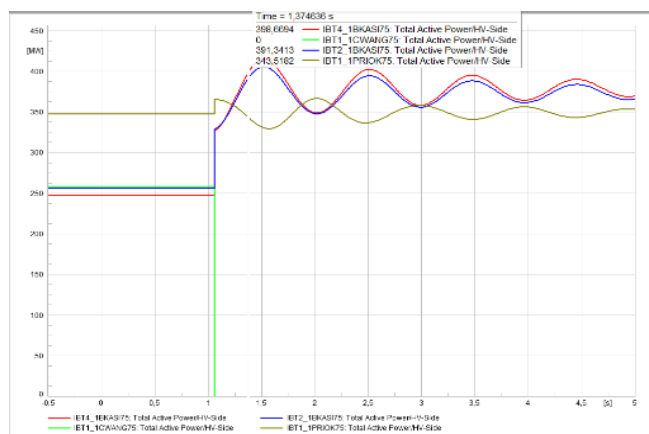


Figure 12. OLS Relay IBT 2,4 Bekasi Start to Send Arming

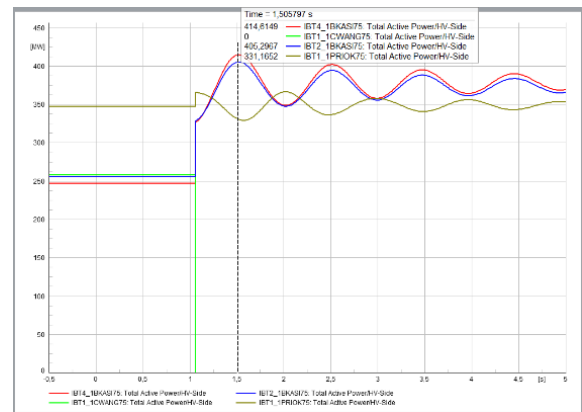


Figure 13. IBT 2,4 Bekasi Reaches Maximum Loading

Regarding the voltage and frequency test results for substations with a vulnerability index >0.5 and generator rotor angles within the normal range, they were consistent with the Contingency N-1 IBT Bekasi test results. The test result graphs can be seen in Figures 14, 15, and 16

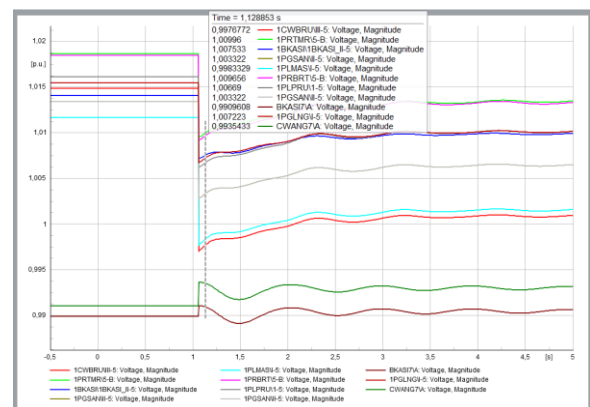


Figure 14. Voltage Values at Substations With a Vulnerability Index > 0.5

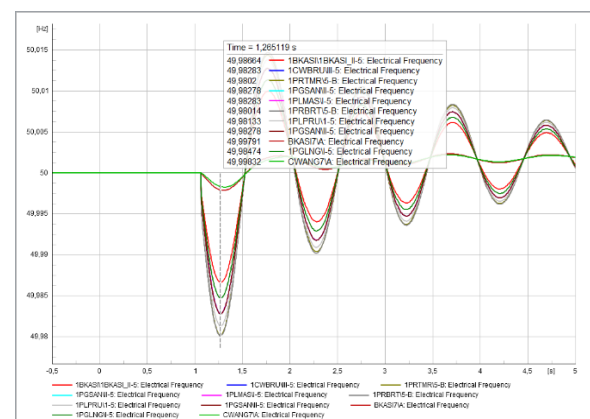


Figure 15. Frequency Values at Substations with a Vulnerability Index > 0.5

Figure 16. Rotor Angles at Priok Generation

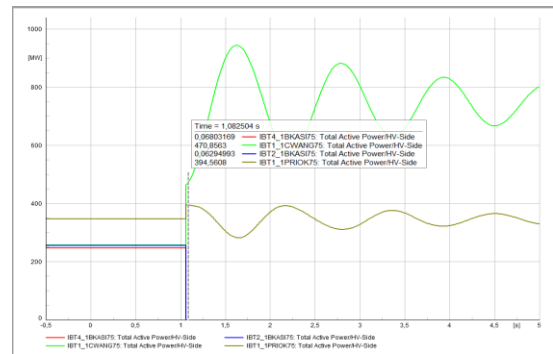
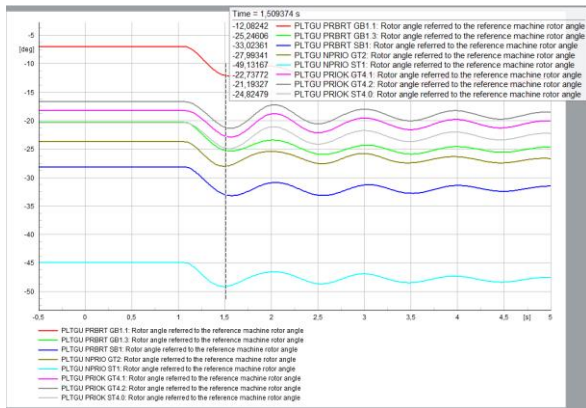


Figure 17. OLS Relay IBT 1 Priok Start to Send Arming and IBT 1 Cawang Overload

A holistic simulation was also performed for the N-1 contingency of IBT 1 Cawang under peak, average, and low load conditions, as shown in Table 8.

Tabel 8. Load Condition Contingency N-1 IBT 1 Cawang Simulation

Load Condition	Total Load SS Priok (MW)	Total Priok SS Generation (MW)	Power Loss (N-1 IBT 1 Cawang) (MW)	OLS (MW)	Final Beban SS (MW)
Peak Load	1109,31	1358,4848	255,7352	205,9939	903,316
Average Load	1063,199	1169,83872	238,3543	0	1063,2
Low Load	702,0316	884,14685	144,1532	0	702,032

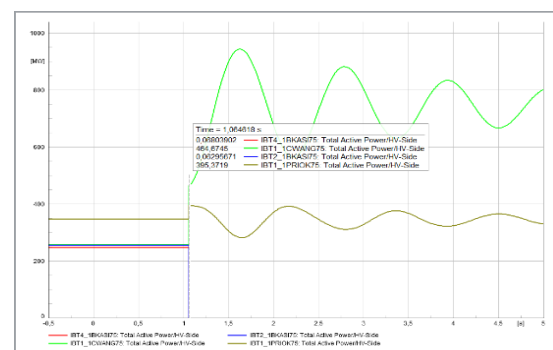


Figure 18. The OCR relay trips IBT 1 Cawang

3.2 N-2 Contingency Simulation

The N-2 Contingency test is crucial as it demonstrates the response of the 150 kV Priok Subsystem to a fault involving two major components, specifically the tripping of IBT 2 and IBT 4 Bekasi. The IBT 2 and 4 Bekasi tripping simulation was conducted at $t_1 = 1.06$ s, resulting in the significant transfer of the total load from IBT Bekasi to IBT Cawang and IBT Priok. At $t_2 = 1.066$ s, as shown in Figure 17, the IBT Priok loading reached 395.3056 MW, triggering the IBT Priok OLS relay to send an arming signal to the ADS Controller. Simultaneously, the IBT Cawang loading reached 464.6745 MW, causing the ADS controller to directly initiate Load Shedding at the prioritized load matrix of IBT Cawang to ensure the integrity of critical equipment such as generators, transmission lines, and IBT Priok within the 150 kV Priok Subsystem. Without successful ADS operation, as observed at $t_3 = 1.085$ s in Figure 18, with IBT Cawang loading at 470.8563 MW, the OCR relay would detect an Over Current condition. This would lead to significant losses for PLN and its consumers as the subsystem would lose three IBTs directly, impacting IBT 1 Priok. If IBT 1 Priok also trips, it would then result in the tripping of Priok Power Plant Blocks 1 and 2 due to the activation of the Over Generating Shedding relay.

For other electrical quantities, significant changes occurred, notably in voltage. Before the fault, the average substation voltage was 1.01 pu; however, post-fault, the voltage decreased to 0.99 pu, as shown in Figure 19. This behavior remains within normal operational limits, as all Automatic Voltage Regulator (AVR) and Governor systems of the Priok Combined Cycle Power Plant (PLTGU) Blocks 1, 3, and 4 operated effectively, with the average rotor angle of the Priok PLTGU units decreasing by 12 degrees, as illustrated in Figure 20. Furthermore, the frequency did not exhibit a significant drop; the lowest recorded frequency remained at 49.91 Hz, preventing the Under Frequency Relays (UFR) from triggering the tripping of main equipment, as depicted in Figure 21.

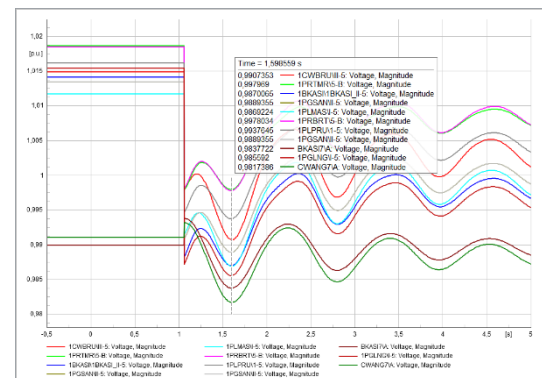


Figure 19. Voltage Values at Substations With a Vulnerability Index > 0.5

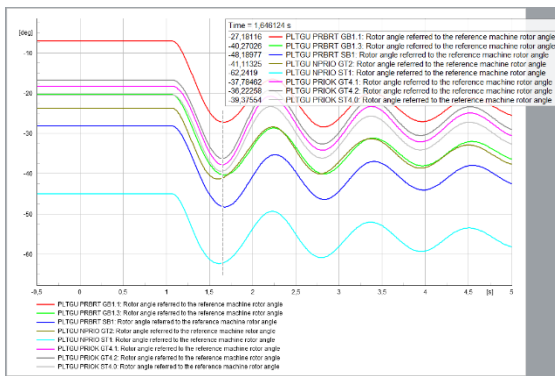


Figure 20. Rotor Angles at Priok Generation

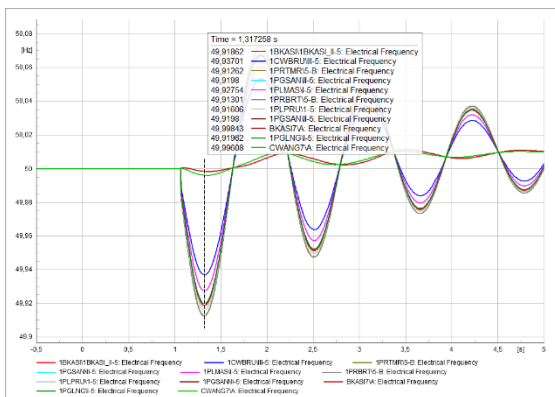


Figure 21. Frequency Values at Substations with a Vulnerability Index > 0.5

The N-2 Bekasi contingency test results across all load conditions indicate that if this occurs, the 150 kV Priok Subsystem would have to shed half of its current total load. This is an event that PT. PLN (Persero) must avoid, as it could potentially lead to Priok, Cawang, and Bekasi islanding conditions. Therefore, PLN must maximize the integration of connections with the 500/150 kV Muara Tawar Subsystem to add 2 IBTs from the Muara Tawar Extra High Voltage Substation (GITET). This would result in a total of 6 IBTs within the 150 kV Priok Subsystem. The results of the N-2 contingency test are presented in Table 9.

Tabel 9. Load Condition Contingency N-2 IBT 2,4 Bekasi Simulation

Load Condition	Total Load SS Priok (MW)	Total Priok SS Generation (MW)	Power Loss (N-1 IBT 1 Cawang) (MW)	OLS (MW)	Final Beban SS (MW)
Peak Load	1109,3101	1358,4848	503,0417	583,0881	526,222
Average Load	1063,1988	1169,83872	460,6891	582,1271	481,0717
Low Load	702,0316	884,14685	277,2895	360,3535	341,6781

VI. CONCLUSION

This study demonstrated that implementing Overload Shedding (OLS) and Adaptive Defense Scheme (ADS) in the 150 kV Priok subsystem significantly enhances Jakarta’s electricity reliability under N-1/N-2 contingency scenarios. Using

DigSILENT PowerFactory, simulations validated that OLS-ADS effectively mitigated cascading failures by dynamically shedding 6–20% of the load during N-1 events (e.g., IBT2/Bekasi or IBT1/Cawang tripping), maintaining voltages (0.9–1.0 pu) and frequencies (49.9–50 Hz) within safe limits. Rotor angles in Priok’s PLTGU units remained stable, adhering to IEEE thresholds. However, N-2 contingencies (e.g., simultaneous loss of IBT2/4/Bekasi) exposed systemic vulnerabilities, requiring 50% load shedding to prevent equipment tripping and islanding.

The research achieved its objective by optimizing ADS logic to prioritize critical loads and generators, ensuring equipment safety during severe faults. Findings underscore the necessity of reinforcing grid infrastructure, such as integrating Muara Tawar’s 500/150 kV IBTs, to bolster N-2 resilience. This work provides actionable insights for refining ADS parameters and expanding transmission capacity, thereby safeguarding Jakarta’s power supply against cascading failures and enhancing system robustness.

REFERENCES

- [1] R. Benato, G. Gardan, and L. Rusalen, “A Three-Phase Power Flow Algorithm for Transmission Networks: A Hybrid Phase/Sequence Approach,” *IEEE Access*, vol. 9, pp. 162633–162650, 2021, doi: 10.1109/ACCESS.2021.3131778.
- [2] B. B. Adetokun, C. M. Muriithi, and J. O. Ojo, “Voltage stability assessment and enhancement of power grid with increasing wind energy penetration,” *Int. J. Electr. Power Energy Syst.*, vol. 120, no. March 2020, p. 105988, 2020, doi: 10.1016/j.ijepes.2020.105988.
- [3] P. D. Putra and M. P. Marbun, “Adaptive Defense Scheme Implementation in Muarakarang Subsystem to Prevent Island Operation Failure,” *Proc. - 11th Electr. Power, Electron. Commun. Control. Informatics Semin. EECCIS 2022*, pp. 88–93, 2022, doi: 10.1109/EECCIS54468.2022.9902921.
- [4] A. W. Ahmad Brian Ikhsana Putra, K. M. Banjarnahor, and N. Hariyanto, “Advanced Technology Implementation of Adaptive Defense Scheme in South and Central Kalimantan System,” *6th Int. Conf. Power Eng. Renew. Energy, ICPERE 2024 - Proc.*, 2024, doi: 10.1109/ICPERE63447.2024.10845441.
- [5] B. Barac, M. Krpan, T. Capuder, and I. Kuzle, “Modeling and Initialization of a Virtual Synchronous Machine for Power System Fundamental Frequency Simulations,” *IEEE Access*, vol. 9, pp. 160116–160134, 2021, doi: 10.1109/ACCESS.2021.3130375.

- [6] PLN, “Buku Defense Scheme UP2B DKI Jakarta dan Banten,” *PT PLN*, vol. 12, no. 1, p. 224, 2024.
- [7] S. K. Samanta and C. K. Chanda, “Stability analysis in a smart grid network due to dynamic demand load respond,” *2017 Int. Conf. Comput. Electr. Commun. Eng. ICCECE 2017*, pp. 1–5, 2017, doi: 10.1109/ICCECE.2017.8526208.
- [8] M. Zare Oskouei, H. Mehrjerdi, D. Babazadeh, P. Teimourzadeh Baboli, C. Becker, and P. Palensky, “Resilience-oriented operation of power systems: Hierarchical partitioning-based approach,” *Appl. Energy*, vol. 312, no. January, p. 118721, 2022, doi: 10.1016/j.apenergy.2022.118721.
- [9] H. Verdejo, V. Pino, W. Kliemann, C. Becker, and J. Delpiano, “Implementation of particle swarm optimization (PSO) algorithm for tuning of power system stabilizers in multimachine electric power systems,” *Energies*, vol. 13, no. 8, 2020, doi: 10.3390/en13082093.
- [10] E. Mancini, M. Longo, W. Yaici, and D. Zaninelli, “Assessment of the Impact of Electric Vehicles on the Design and Effectiveness of Electric Distribution Grid with Distributed Generation,” *Appl. Sci.*, vol. 10, no. 15, 2020, doi: 10.3390/app10155125.
- [11] H. Khoshkhoo, S. Yari, A. Pouryekta, V. K. Ramachandaramurthy, and J. M. Guerrero, “A Remedial Action Scheme to Prevent Mid/Long-Term Voltage Instabilities,” *IEEE Syst. J.*, vol. 15, no. 1, pp. 923–934, 2021, doi: 10.1109/JSYST.2020.3010781.
- [12] R. Małkowski, M. Izdebski, and P. Miller, “Adaptive algorithm of a tap-changer controller of the power transformer supplying the radial network reducing the risk of voltage collapse,” *Energies*, vol. 13, no. 20, 2020, doi: 10.3390/en13205403.
- [13] J. Andruszkiewicz, J. Lorenc, B. Staszak, A. Weychan, and B. Zięba, “Overcurrent protection against multi-phase faults in MV networks based on negative and zero sequence criteria,” *Int. J. Electr. Power Energy Syst.*, vol. 134, 2022, doi: 10.1016/j.ijepes.2021.107449.
- [14] J. Boyle, T. Littler, S. M. Muyeen, and A. M. Foley, “An alternative frequency-droop scheme for wind turbines that provide primary frequency regulation via rotor speed control,” *Int. J. Electr. Power Energy Syst.*, vol. 133, no. March, p. 107219, 2021, doi: 10.1016/j.ijepes.2021.107219.
- [15] B. Huang and J. Wang, “Applications of Physics-Informed Neural Networks in Power Systems - A Review,” *IEEE Trans. Power Syst.*, vol. 38, no. 1, pp. 572–588, 2023, doi: 10.1109/TPWRS.2022.3162473.
- [16] C. Sun *et al.*, “Design and Real-Time Implementation of a Centralized Microgrid Control System with Rule-Based Dispatch and Seamless Transition Function,” *IEEE Trans. Ind. Appl.*, vol. 56, no. 3, pp. 3168–3177, 2020, doi: 10.1109/TIA.2020.2979790.
- [17] X. Hu, H. Hu, S. Verma, and Z. L. Zhang, “Physics-Guided Deep Neural Networks for Power Flow Analysis,” *IEEE Trans. Power Syst.*, vol. 36, no. 3, pp. 2082–2092, 2021, doi: 10.1109/TPWRS.2020.3029557.
- [18] A. Ahlawat and S. T. Nagarajan, “Study of estimating dynamic state jacobian matrix and dynamic system state matrix based on PMU,” *2020 IEEE Int. Conf. Comput. Power Commun. Technol. GUCON 2020*, no. 3, pp. 614–618, 2020, doi: 10.1109/GUCON48875.2020.9231185.
- [19] D. R. Alwaini and H. S. Dini, “Design of Defense Scheme Based on Adaptive under Frequency Load Shedding (AUFLS) at Lombok Island Grid System,” *2021 3rd Int. Conf. High Volt. Eng. Power Syst. ICHVEPS 2021*, pp. 117–121, 2021, doi: 10.1109/ICHVEPS53178.2021.9601026.
- [20] PLN, “SPLN S5.005: Sistem Defense Scheme,” *PT PLN*, 2022.